Generation of Orthogonal, Boby-Fitted Grids Using Potential Flow Solution by the Panel Method

By

Masanori HAYASHI*, Akira SAKURAI* and Masashi NAGAHATA*

(February 1, 1983)

Summary: A new method of generating an orthogonal, body-fitted grid is presented. It uses the equi-potential lines and the streamlines in an imaginary, potential flow around a body calcutated by the panel method as the grid lines. The computation is stable and grid density control is easy to achieve. It may also be extended to the generation of the so-called C-grids.

1. Introduction

When applying the finite-difference method to the solution of flow fields around bodies with arbitrary shapes, it is necessary to introduce some kind of coordinate change which transforms an equi-spaced calculation grid to a curvilinear grid system which is tangent to the body surface. This problem of generating the so-called body-fitted grid has seen great advances in recent years, and many useful methods have been proposed [1]–[5].

Most known among them is the method due to Thompson, Thames and Mastin [2]–[5], which is based on solving elliptic partial differential equations describing the transformation by a finite-difference method. The grid-point density control is achieved by controlling the forcing terms in the Poisson equation, which seems to need much experience. Moreover, the resulting grid is not orthgonal.

For fluid dynamicist, the system of equi-potential lines and streamlines in the potential flow around a body constitutes the most familiar example of an orthogonal, curvilinear grid. The potential flow around a body, in return, can be calculated explicitly using the panel method. We have combined these two ideas to obtain a new method of generating an orthogonal, density controllable, bodyfitted grid.

2. Method of Grid Generation

(A) Outline of the Method

The sequence of coordinate transformations is shown schematically in Fig. 1. Let us represent the velocity potential and the stream function of the inviscid flow around the body by α and β respectively. Note that the potential flow treated here is purely imaginary, used only to generate the grid system and has no relation to the physical flow to be solved using the generated grid.

* Department of Aeronautical Engineering, Kyushu University

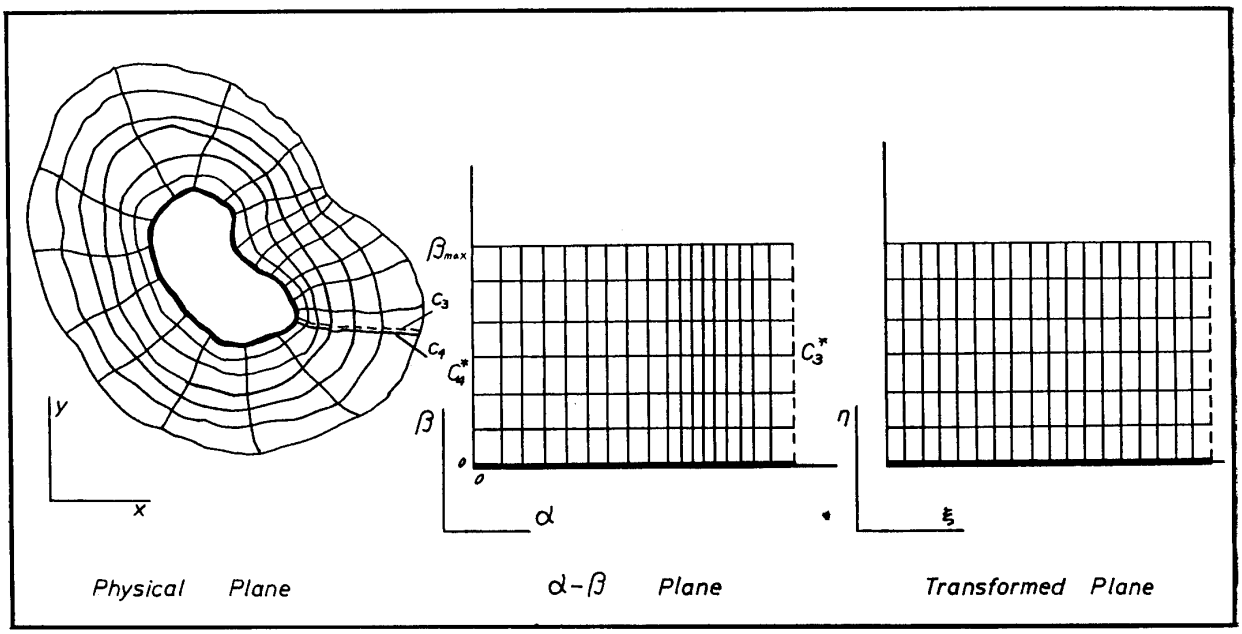

Fig. 1. Steps of coordinate transformation.

The first step of grid generation is to obtain the potential flow solution. Although the finite-difference method may be used to do it, the simpler way is to use the panel method, in which the body is represented by a polygon with singularity distribution on its sides and the flow around it is determined by solving for the strength of the singularity so as to satisfy the boundary conditions on the control points placed one on each side of the polygon.

After the potential flow is determined, constant α and β values constitute rectangular grid lines in the $\alpha-\beta$ plane. It is more useful for practical purposes, however, to apply one more stage of transformation independently to α and β and make the final $\xi-\eta$ plane the calculation plane. The transformation relation can be arbitrarity chosen so as to obtain some measure of grid-point density control.

Thus the grid generation is achieved by the following steps:

i) The potential flow around the body is solved by the panel method.
ii) The grid density control transformation $\xi=\xi(\alpha)$, $\eta=\eta(\beta)$ is chosen.
iii) For each grid point in the $\xi-\eta$ plane, the corresponding $x-y$ coordinates are traced.
iv) Steps ii) and iii) are repeated, if necessary, until the desired grid configuration is obtained.

(B) Solution of the Potential Flow

Let us consider a problem of a potential flow outside a single body in an open space for simplicity, although multiple bodies or a body in a closed space may be treated similarly. It is also convenient to use the complex velocity potential formulation, since complex calculation is available in Fortran.

The body is approximated by a polygon, whose Nr vertices are denoted by position vectors $z_1, z_2, \cdots, z_{Nr}$ and the sides by vectors

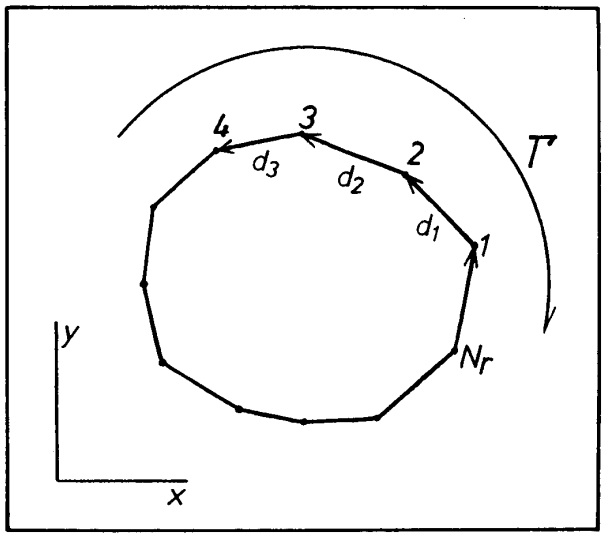

Fig. 2. Notation concerning the body approximation.

$$d_j=z_{j+1}-z_j\,;\quad j=1\sim N_r \tag{1}$$

as in Fig. 2. In the following expressions, suffix $Nr+1$ means 1 and 0 means Nr. A vortex sheet with linearly varying strength per unit length

$$\gamma(s)=\gamma_j+(\gamma_{j+1}-\gamma_j)s\,;\qquad 0\leq s\leq 1 \tag{2}$$

is assumed on each side d_j of the polygon. The velocity vector induced by all of these vortex sheet at a point z_c is

$$q_c=\sum_{j=1}^{Nr}A_j\gamma_j \tag{3}$$

where

$$A_j=\frac{i}{2\pi}\{|d_{j-1}|[d_{j-1}I_{2_{j-1}}-z_cI_{1_{j-1}}]-|d_j|[d_jI_{2_j}-(z_c+d_j)I_{1_j}+z_cI_{0_j}]\} \tag{4}$$

and the integrals I_{0_j} through I_{2_j} are given as

$$\begin{aligned}
I_{0_j}&=\frac{1}{|d_jz_c\sin\delta|}\left\{\tan^{-1}\left[\frac{1}{|\sin\delta|}\left(\left|\frac{d_j}{z_c}\right|-\cos\delta\right)\right]+\tan^{-1}\frac{\cos\delta}{|\sin\delta|}\right\}\\
I_{1_j}&=\frac{1}{|d_j|^2}\log\left|\frac{d_j-z_c}{z_c}\right|+\left|\frac{z_c}{d_j}\right|\cos\delta\cdot I_{0_j}\\
I_{2_j}&=\frac{1}{|d_j|^2}+2\left|\frac{z_c}{d_j^3}\right|\cos\delta\cdot\log\left|\frac{d_j-z_c}{z_c}\right|+\left|\frac{z_c}{d_j}\right|^2(2\cos^2\delta-1)I_{0_j}\\
\delta&\equiv\mathrm{Arg}\frac{z_c}{d_j}
\end{aligned} \tag{5}$$

when the point z_c is neither on the side d_j nor on its extention, or as

$$
\begin{aligned}
I_{0j} &= -\frac{1}{|d_j|^2}\frac{1}{(1-\kappa_j)\kappa_j} \\
I_{1j} &= \frac{1}{|d_j|^2}\log\left|\frac{1-\kappa_j}{\kappa_j}\right| + \kappa_j I_{0j} \\
I_{2j} &= \frac{1}{|d_j|^2} + \frac{2\kappa_j}{|d_j|^2}\log\left|\frac{1-\kappa_j}{\kappa_j}\right| + \kappa_j^2 I_0 \\
\kappa_j &\equiv \frac{z_c}{d_j}
\end{aligned}
\qquad (6)
$$

otherwise.

The normal velocity component q_{n_i} at the control point z_{c_i} placed at the mid-points of each side, d_i, is

$$
q_{n_i} = \sum_{j=1}^{Nr} \langle n_{c_i} \cdot A_j \rangle \gamma_j \qquad (7)
$$

where n_{c_i} is the unit outward normal vector and $\langle\ \rangle$ means the inner product.

The boundary condition is that the normal velocity component given by Eq. (7), or by the sum of Eq. (7) and the normal component of the uniform flow when it is superposed, vanishes at every control point. This gives rise to a system of Nr linear equations in γ_1 through γ_{Nr}. Since the total circulation must be specified, as unity for example, there remains only $Nr-1$ independent variables for the Nr boundary conditions. One method to solve this redundancy would be to omit some control point from the system of equations. This it not satisfactory for the present purpose since small but finite residual normal velocity is observed at the omitted control point when Nr is finite. Instead we have chosen to evaluate the boundary condition at every control point and include the residual, constant normal velocity component itself, U_{n_0}, into the system of equations. This has the effect of distributing the discretization error on all control points. U_{n_0} tends to zero when Nr tends to infinity.

(C) Grid Tracing

As the first step for tracing grid lines, formulations must be obtained for the velocity potential, α, and the stream function, β, induced by the calculated vorticity distribution.

The value of the stream function which one vortex sheet induces at a point z_c is

$$
\beta_j = \frac{|d_i|}{4\pi}[\gamma_j J_{0j} + (\gamma_{j+1} - \gamma_j) J_{1j}] \qquad (8)
$$

where the integrals J_{0j} and J_{1j} are

$$
\begin{aligned}
J_{0j} &= \frac{1}{|d_j|}[x\log(x^2+C) - 2x + 2CI_A]_{x_0}^{x_1} \\
J_{1j} &= \frac{1}{2|d_j|^2}[(x^2+C)\log(x^2+C) - x^2]_{x_0}^{x_1} + \left|\frac{z_c}{d_j}\right|\cos\delta \cdot J_{0j}
\end{aligned}
\qquad (9)
$$

and

$$C \equiv |z_c|^2 \sin^2 \delta$$

$$I_A \equiv \begin{cases} \dfrac{1}{\sqrt{C}} \tan^{-1} \dfrac{x}{\sqrt{C}} & \cdots C>0 \\ -\dfrac{1}{x} & \cdots C=0 \end{cases} \tag{10}$$

$$x_0 \equiv -|z_c| \cos \delta$$

$$x_1 \equiv |d_j| \left(1 - \left|\frac{z_c}{d_j}\right| \cos \delta\right)$$

The total stream function at a point is determined by summing Ex. (8) for $j=1$ to N_r except for an arbitrary additive constant. These constants in β and also in α are determined when α and β values at some point z are specified. Usually $\alpha=1.0$ and $\beta=0$ are specified at the control point, z_{c_1}.

The velocity potential, α_j, induced at z_c by the vortex sheet on d_j is given by

$$\alpha_j = -\frac{|d_j|}{2\pi}\left[(\gamma_j+(\gamma_{j+1}-\gamma_j)b)\left\{\tau+\theta_0 b-\theta_1(b-1)+\frac{1}{2}h \log\frac{h^2+b^2}{h^2+(b-1)^2}\right\}\right.$$
$$\left.-(\gamma_{j+1}-\gamma_j)\left\{\frac{2b-1}{2}\tau+\frac{1}{2}[\theta_0(h^2+b^2)-\theta_1(h^2+(b-1)^2)]+\frac{h}{2}\right\}\right] \tag{11}$$

where τ and θ refer to the angles as shown in Fig. 3(a), and h and b as shown in Fig. 3(b) in d_j oriented coordinates.

It can be shown from Eq. (11) that there appears a potential jump of $|d_j|(\gamma_j+\gamma_{j+1})/2$ when θ moves across the negative real axis. This corresponds to the fact that the velocity potential outside a body with circulation is a multi-valued function. In order to keep α single-valued, the grid point where α is evaluated must be moved in some regular manner in the $x-y$ plane, and whether θ crossed

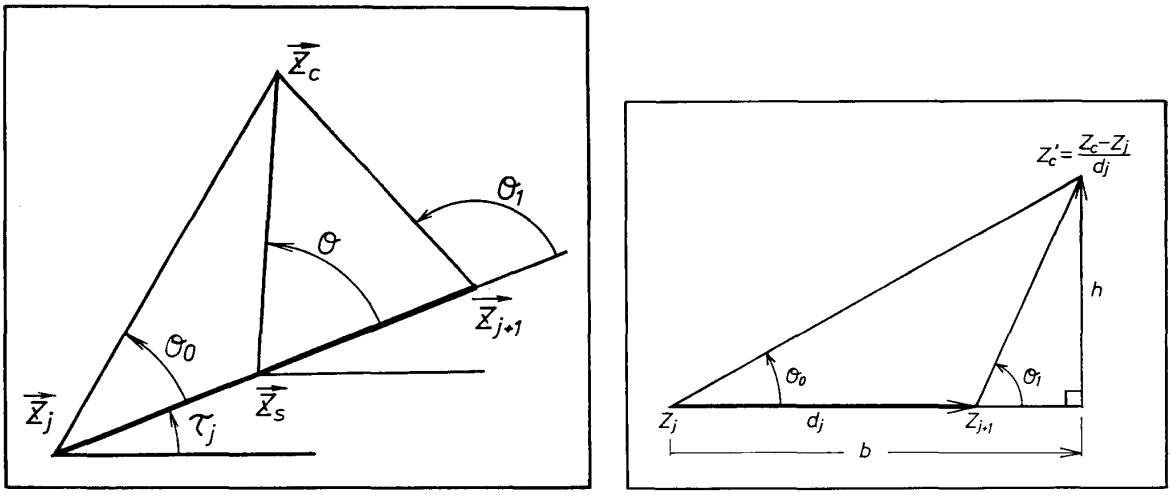

(a) Relative angles (b) Angles and lengths relative to d_j

Fig. 3. Notation for potential calculation.

the negative real axis or not must be decided for each d_j from the movement of the point. The potential jump is then compensated for if necessary.

The next step of grid point tracing is to obtain some iteration scheme for x and y, since what is really needed is the values of x and y for a specified set of α and β, not vice versa. The Newton-Raphson iteration in two variables has been found suitable for this purpose.

In practice, the $\alpha=1$ equi-potential line extending outward from z_c, is treated first, then each streamline starting from it is traced counterclockwise around the body. The grid points on the body wall must be treated separately, since calculated α and β are good approximations only at the control points and show singular behavior at the vertices. This difficulty is avoided by linearly interpolating between the function values at neighboring control points when a grid point is on the body surface.

(D) Calculation of the Metric Parameters

In order to perform finite-difference calculations, not only the $x-y$ coordinates but other metric parameters such as $h^2=(\partial\alpha/\partial x)^2+(\partial\alpha/\partial y)^2$, $\partial^2\alpha/\partial x\partial y$, $\partial^2\alpha/\partial x^2$ must be known at each grid point. The second derivatives of α (those for β are obtained from them by the Cauchy-Riemann equations) are obtained as

$$\frac{\partial^2\alpha}{\partial x^2}=\mathrm{Re}\left(\frac{d^2f}{dz^2}\right),\qquad \frac{\partial^2\alpha}{\partial x\partial y}=-\mathrm{Im}\left(\frac{d^2f}{dz^2}\right) \tag{12}$$

where f is the complex velocity potential. The second derivative of f can be easily determined from the formulation in 2(B).

3. Applications and Extensions

Figures 4 through 8(a) show examples of grids generated by this method, while Fig. 8(b) shows streamlines around an NACA 0015 airfoil at Re=20 calculated by the $N-S$ equations with the grid in Fig. 8(a). Experiences with this generation method have shown that the method is easy to use with any kind of body shape because it is free from instability phenomenon as the potential solution is obtained explicitly, and that the grid point clustering through $\alpha-\beta$ to $\xi-\eta$ transformation is easy to realize.

The computation time requirement, however, is not small from two reasons: 1) the grid point coordinates must be determined iteratively; 2) the number of vertices, Nr, must be much larger than the number of grid points along the body wall, since the wall values must be obtained by linear interpolation between control point values. The computation time needed to trace the grid lines may be shortened to about one third by replacing the vortex sheet with a point vortex with the same circulation placed at the centroid of the vorticity distribution. At present, it takes about 20 seconds of CPU time of FACOM M-200 to trace a 40-by-15 grid after the above modification.

All the grids shown so far are the so-called O-grids. The so-called C-grids are more useful for many applications like the airfoil calculations. This may be

generated by placing another body with the same shape in the mirror-image position and connecting them with a vortex sheet as shown schematically in Fig. 9. The strength and vertical location of the vortex sheet are determined from two conditions: 1) the normal velocity component at the control point on the vortex sheet segment must be zero; 2) If $\alpha=\alpha_l$ on the lower surface of the vortex sheet

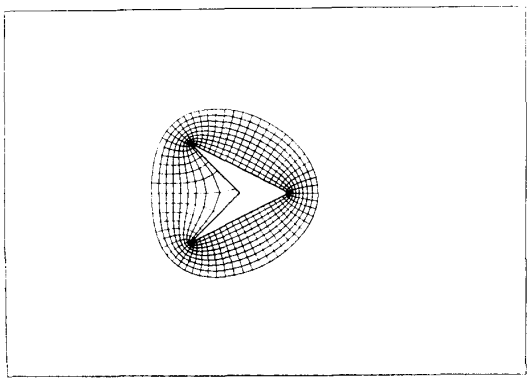

Fig. 4. Grid around a body with convex and concave corners.

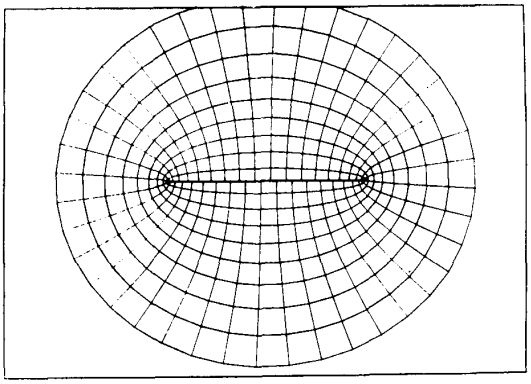

Fig. 5. Grid around a flat plate.

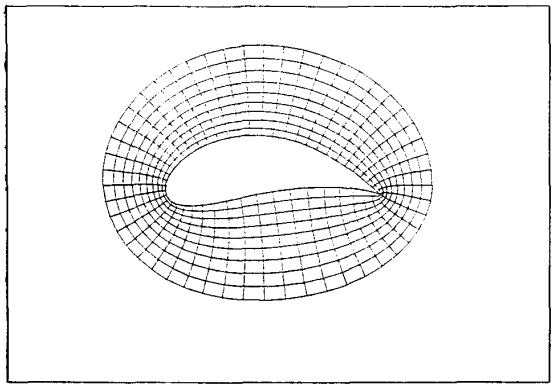

Fig. 6. Grid around a Kármán-Trefftz wing

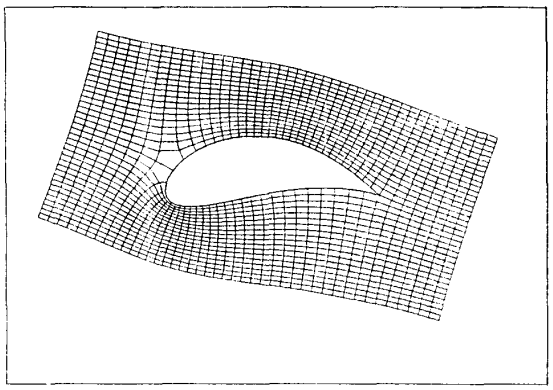

Fig. 7. Grid around a Kármán-Trefftz wing with Superposed Freestream.

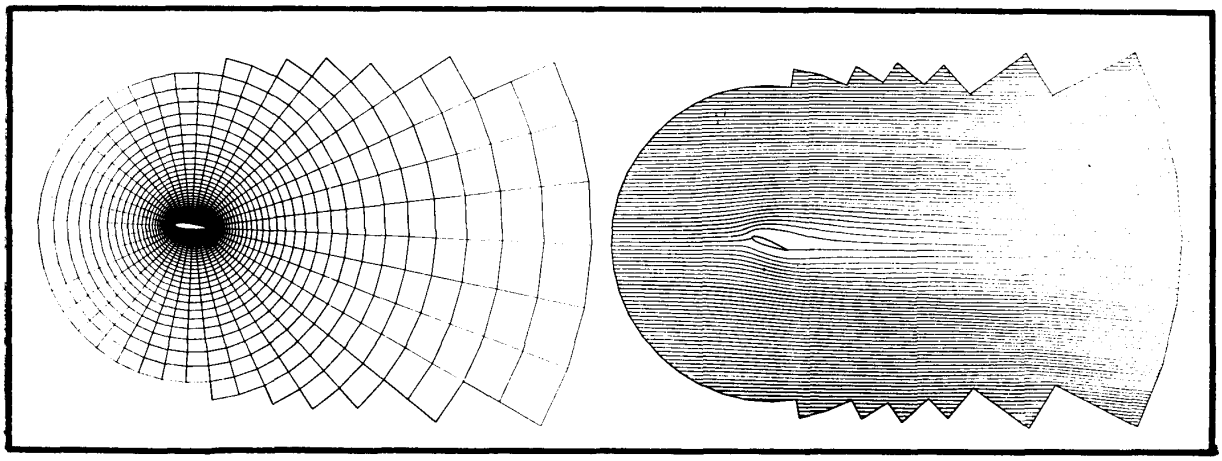

(a) Grid around an NACA 0015 airfoil

(b) Re=20 Streamlines around it by N-S calculation

Fig. 8. Application on the airfoil calculation.

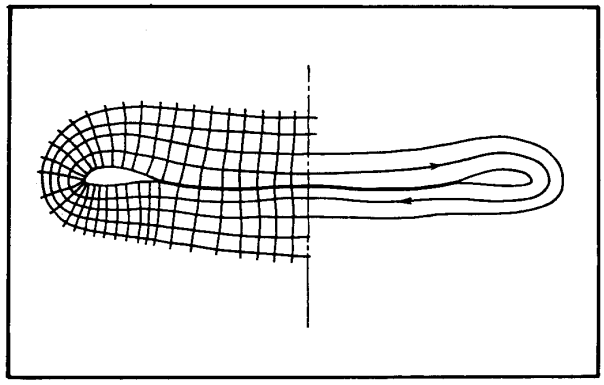

Fig. 9. Method of generating a C-grid.

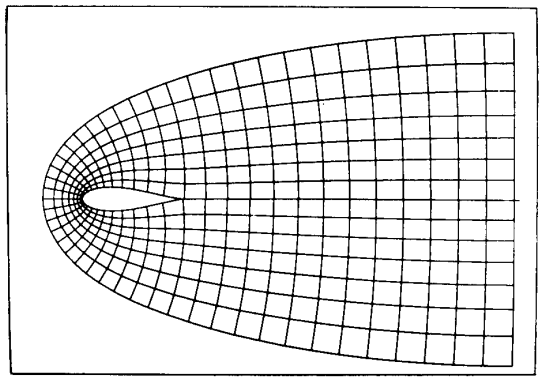

Fig. 10. An example of a C-grid.

at the control point, that on the upper surface must be $1-\alpha_l$, when total circulation left of the origin is 1.0. The latter guarantees that the resulting $\alpha=$constant grid lines are continuous across the vortex sheet, which is essential for the application of the periodicity condition there.

Fig. 10 shows one example of such a grid. The present algorithm for determining the free vortex sheet configuration needs further improvements, however, and a small amount of discontinuity of α-lines across the vortex sheet is observed in the figure. Moreover, the configuration of the grid shown in Fig. 10 is not completely satisfactory since the β-lines fan out fairly rapidly downstream of the body. The density control through $\alpha-\beta$ to $\xi-\eta$ transformation is not effective enough. Further control may be possible if the bodies should be placed in a closed space and the shape of the external boundary should be changed to effect the desired grid-point clustering.

4. Conclusions

A new method of generating orthogonal, body-fitted finite-difference grid which utilizes the solution of the imaginary, inviscid potential flow around the body calculated by the panel method was developed, and its usefulness was shown by several examples of grid generation and Navier-Stokes calculation using it.

The calculation is straightforward since no finite-difference calculation is needed for the grid generation, and the control of the grid-point density is easy.

This method may be extended to the generation of the so-called C-grids.

References

[1] NASA CP-2166, (1980).
[2] Thompson, J. F., Thames, F. C., and Mastin, C. W.: J. Comp. Phys., Vol. 15, (1974), pp. 299-319.
[3] Thames, F. C., Thompson, J. F., Mastin, C. W., and Walker, R. L.: J. Comp. Phys., Vol. 24, (1977), pp. 245-373.
[4] Thompson, J. F., Thames, F. C., and Mastin, C. W.: J. Comp. Phys., Vol. 24, (1977), pp. 274-302.
[5] Thompson, J. F., Thames, F. C., and Mastin, C. W.: NASA CR-2729, (1977).